

## Drag and Lift Estimation from 3-D Velocity Field Data Measured by Multi-Plane Stereo PIV

Hiroyuki Kato  
Kisa Matsushima  
Makoto Ueno  
Shunsuke Koike  
Shigeya Watanabe

Japan Aerospace Exploration Agency  
Chofu, Tokyo 182-8522  
Japan  
kato.hiroyuki@jaxa.jp

### Abstract

For airplane design, it is crucial to have tools that can accurately predict airplane drag and lift. Usually drag and lift prediction methods are force measurement using wind tunnel balance. Unfortunately, balance data do not provide information contribution of airplane to components to drag and lift for more precise and competitive airplane design. To obtain such information, a wake integration method for use drag and lift estimation was developed for use in wake survey data analysis. Wake survey data is commonly measured by multi-hole pressure probes. But pressure probe measurement requires considerable time, so that it is difficult to apply many conditions in wind tunnel testing. On the other hand, PIV measurement possesses the ability to acquire velocity distribution data at relatively short times. However, PIV measurement does not provide pressure data directly. Therefore, the pressure estimation technique is developed to enhance the value of PIV data. The technique conducts computational fluid dynamics (CFD) computation to estimate pressure field using multi-plane stereo PIV velocity data. Finally, drag and lift profiles are predicted by the wake integration method using velocity data measured by PIV and pressure data estimated by CFD.

Key words: Wind Tunnel Testing, Flow Measurements, Wake, PIV

### Introduction

In general, the aerodynamic forces exerted on a wind tunnel test model are obtained using an aerodynamic force balance, which measures the integrals of pressure and friction on the model's surface and gives a near-field representation of the aerodynamic forces. Wake integration method is an attractive tool both for wind tunnel testing and CFD analysis, mainly because it can render the spanwise distribution of drag and lift visible quantitatively, and this knowledge of the aerodynamic force distribution is useful for drag source identification. Additionally, it can decompose drag into induced drag and profile drag components. Drag decomposition gives insight into the flow physics necessary for design improvement. But pressure probe measurement requires considerable time, so that it is difficult to apply many conditions in wind tunnel testing. On the other hand, PIV measurement possesses the ability to acquire velocity distribution data at relatively short times. However, PIV measurement does not provide pressure data directly. Therefore, the pressure estimation technique is developed to enhance the value of PIV data. The technique conducts computational fluid dynamics (CFD) computation to estimate pressure field using PIV velocity data. Finally, drag and lift profiles are predicted by the wake integration method using velocity data measured by PIV and pressure data estimated by CFD. In the verification procedures, this technique were performed of the PIV data of the NACA0012 rectangle wing model in wind tunnel testing, and the drag and lift forces estimated by PIV data directly compared with measured balance data.

## Drag and Lift Prediction Method

The Poisson equation for pressure (equation (1)) is the basic equation for the computation. The equation is derived from the divergence form of three-dimensional incompressible Navier-Stokes equations. It is assumed that velocity gradient in the freestream direction is 0 and a flow is steady. Then the two-dimensional equation is obtained. All terms of the equation are discretized using the 2nd-order central difference method. General coordinates transformation is done for wide applicability of the system. The discretized Poisson equation for pressure which is a simultaneous linear equation system is solved numerically by SOR (successive-over-relaxation) method [2].

$$\frac{\partial^2 p}{\partial y^2} + \frac{\partial^2 p}{\partial z^2} = - \left\{ \left( \frac{\partial v}{\partial y} \right)^2 + 2 \frac{\partial v}{\partial z} \frac{\partial w}{\partial y} + \left( \frac{\partial w}{\partial z} \right)^2 + v \frac{\partial D}{\partial y} + w \frac{\partial D}{\partial z} \right\} + \frac{1}{\text{Re}} \left( \frac{\partial^2 D}{\partial y^2} + \frac{\partial^2 D}{\partial z^2} \right) \quad (1)$$

$$\left( D = \frac{\partial v}{\partial y} + \frac{\partial w}{\partial z} \right)$$

The aerodynamic forces are expressed as the balance of momentum over a control volume around the model. Although the classical far-field method requires the integration of physical properties over the entire surface of the control volume, Betz succeeded in confining the integral to the inside the model's wake for two-dimensional wind tunnel drag measurement, and the theory was extended to three-dimensional wind tunnel testing by Maskell. Maskell's method was epoch-making as it required planar traversing measurement only within the wake of a wind tunnel model to acquire aerodynamic drag and lift forces (Figure 1).

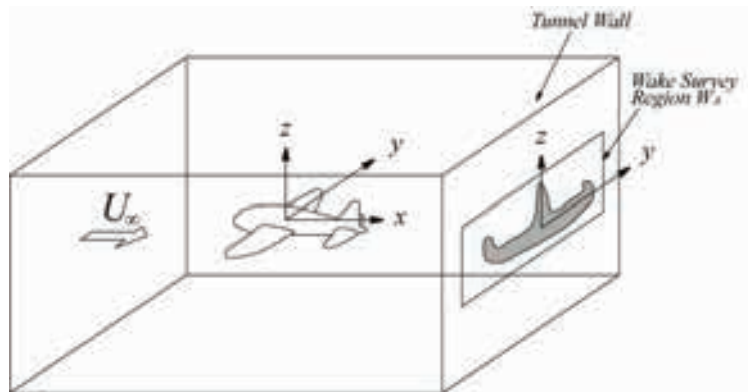


Figure 1 Image of wake integral control volume.

The wake integral method is described by Kusunose[1] in detail. The drag coefficient (CD) is written as

$$CD = CDP + CDI + CDP2 + O(\Delta 3) \quad (2)$$

CDP, CDI, CDP2 are profile drag coefficient, induced drag coefficient, 2nd order profile drag coefficient, respectively. And profile drag coefficient (CDP) is as follows

$$CDP = \frac{\iint_{W_A} P_\infty \frac{\Delta s}{R} dy dz}{\frac{1}{2} \rho_\infty U_\infty^2 S} \quad (3)$$

Denominator in right-hand side is dynamic pressure, and S control volume surface area.  $P_\infty$ ,  $\rho_\infty$ ,  $U_\infty$  are static pressure, density, velocity of freestream, respectively, and  $\Delta s$  is perturbation entropy, R is gas constant. WA is integral area over the model wake region. Induced drag (CDI) is as follows

$$CDI = \frac{\iint_{WA} \psi \xi dy dz}{\frac{1}{2} \rho_\infty U_\infty^2 S} \quad (4)$$

$\xi$  is x-component of vorticity vector, and  $\psi$ ,  $\phi$  two-dimensional stream function, and are as follows

$$v = \frac{\partial \psi}{\partial z} + \frac{\partial \phi}{\partial y}, \quad w = -\frac{\partial \psi}{\partial y} + \frac{\partial \phi}{\partial z} \quad (5)$$

2nd order profile drag is as follows

$$CDP2 = \frac{\iint_{WA} \frac{P_\infty}{2} \left( \frac{\Delta s}{R} \right)^2 dy dz}{\frac{1}{2} \rho_\infty U_\infty^2 S} \quad (6)$$

Lift coefficient is as follows

$$CL = \frac{\rho_\infty U_\infty \iint_{WA} y \xi dy dz - \rho_\infty U_\infty^2 (1 - M_\infty^2) \iint_{WA} \frac{w}{U_\infty} \frac{\Delta s}{U_\infty} ds + M_\infty^2 \frac{\gamma P_\infty}{R} \iint_{WA} \frac{w}{U_\infty} \Delta s ds}{\frac{1}{2} \rho_\infty U_\infty^2 S} \quad (7)$$

## Wind Tunnel Testing

A conventional low-speed wind tunnel with a 2m x 2m test section was used for the present PIV test. A photograph of the wind tunnel model is shown in figure 2. The model is a NACA0012 rectangular wing (chord = 200 mm, span = 1,000 mm). The test was conducted at a freestream velocity  $U_\infty$  of 30.0m/s. Angle of attack ( $\alpha$ ) was set in a range between 0° and 8°.

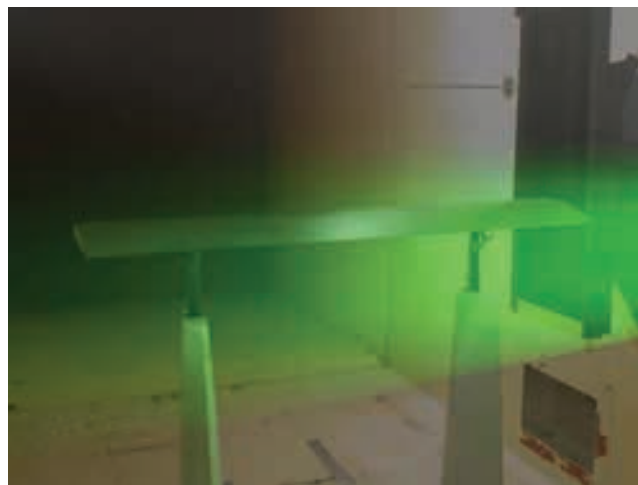
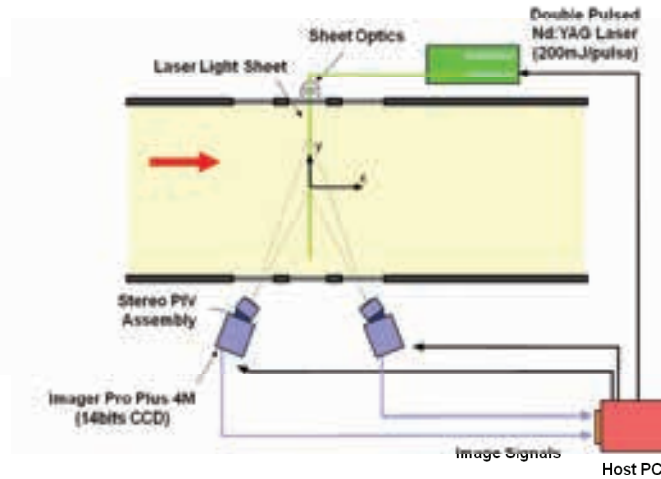


Figure 2 The wind tunnel test model of NACA0012 rectangle wing.

A stereoscopic (3-C) PIV system which has been developed for the JAXA wind tunnels was employed for the present test. In the PIV measurement, the laser light sheet was located perpendicular to the freestream (figure 3).



**Figure 3 Schematic of Stereo PIV setting.**

A stereoscopic (3-C) PIV system which has been developed for the JAXA wind tunnels [3] was employed for the present test. In this measurement, stereoscopic PIV with two cameras with different view angles were performed. Figure 3 shows stereoscopic PIV configuration. In some cases, we employed to measure three components of velocity. In vector processing, we applied several steps of velocity vector validation. After the validation, ensemble instantaneous data at an identical test condition are averaged. Oil droplets with a diameter of around  $1\mu\text{m}$  were used as the seed particles. In the stereoscopic PIV measurement, the sheet was located perpendicular to the free stream. Interrogation spot size is  $32 \times 32$  pixels with 50% overlap. Time separation  $\Delta t$  was set from 45 to 55  $\mu\text{s}$  step by 0.2  $\mu\text{s}$  in order to reduce bias error due to difference of  $\Delta t$ .

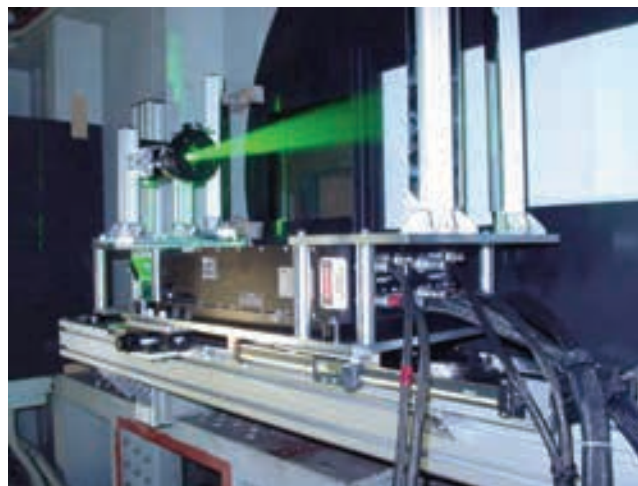


**Figure 4 Laser light sheet optics.**

## Experimental Results

Figure 5 shows three components of velocity distribution measured in the wind-tunnel testing. Color contour shows a velocity component of the freestream direction ( $u$ ).

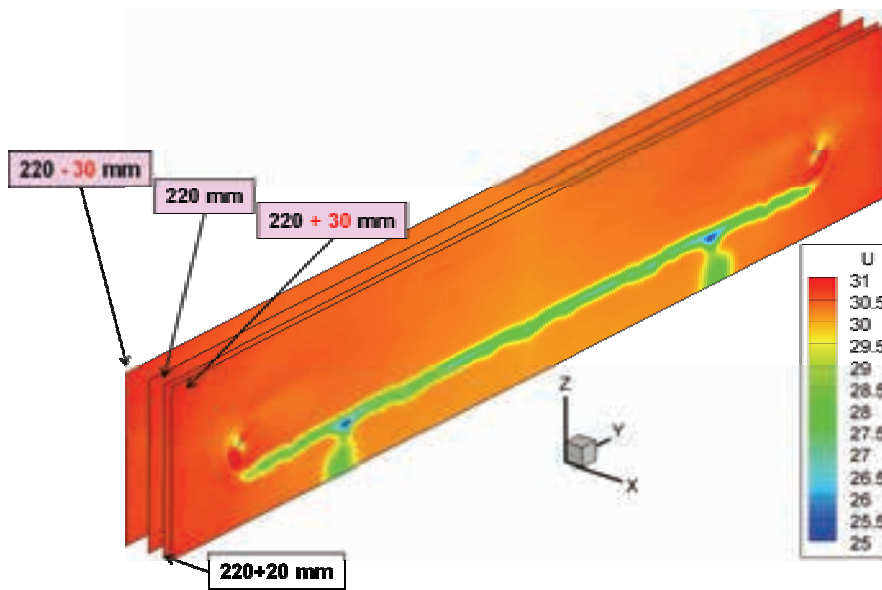


Figure 5 multi-plane stereo PIV results ( $U=30\text{m/s}$ ,  $\text{AoA}=8\text{deg}$ ).

Figure 6 shows pressure distributions estimated from three velocity components by CFD method. In the case of attack of angle 8 degree, it is qualitatively good results that there are low pressure region near a wing tip vortex.

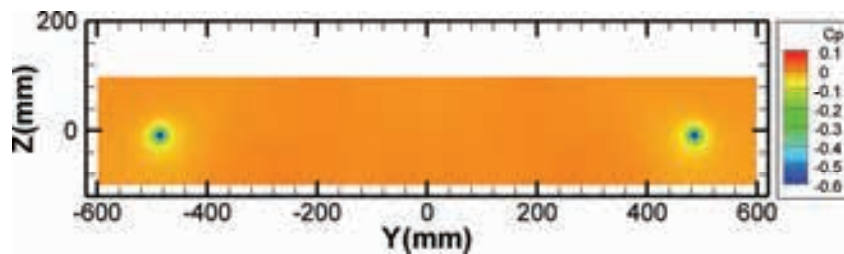


Figure 6 multi-plane stereo PIV results ( $U=30\text{m/s}$ ,  $\text{AoA}=8\text{deg}$ ).

Figure 7 and 8 show profile drag distribution ( $c_{dp}$ ) and induced drag distribution ( $c_{di}$ ), respectively. These results are calculated from three velocity components and pressure distribution at wake region by wake integration method. The computational code developed and validated by Ueno et. al[4] was used applied wake integration method.

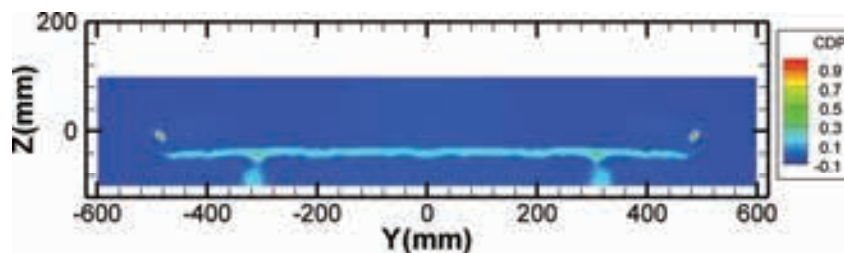


Figure 7 multi-plane stereo PIV results ( $U=30\text{m/s}$ ,  $\text{AoA}=8\text{deg}$ ).

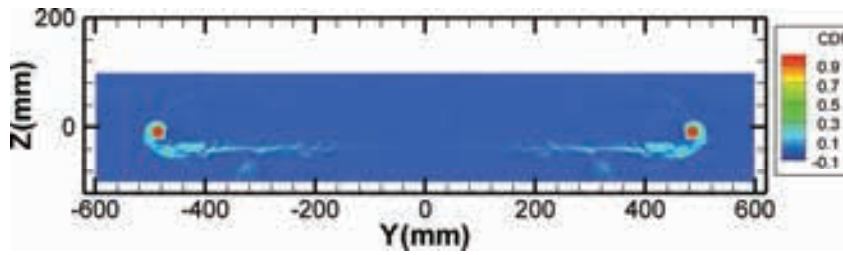


Figure 8 multi-plane stereo PIV results (U=30m/s, AoA=8deg).

In the profile drag distribution, there are large drag components at the model and model supports. On the other hand, in the induced drag distribution, there are peaks of profile drag near the tip vortex at attack of angle 8 degree.

Figure 9, 10 and 11 show profile drag, induced drag and lift distributions in spanwise direction, respectively. Also in the spanwise distributions, profile and induced drag denote the same tendency of the distributions in the wake plane. In the lift distribution, it is fairly good results that there is a peak at center of the wing span.

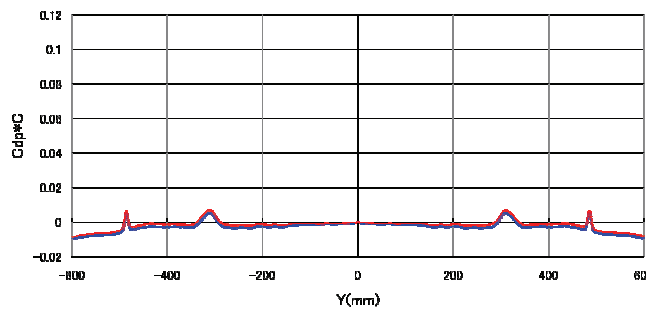


Figure 9 multi-plane stereo PIV results (U=30m/s, AoA=8deg).

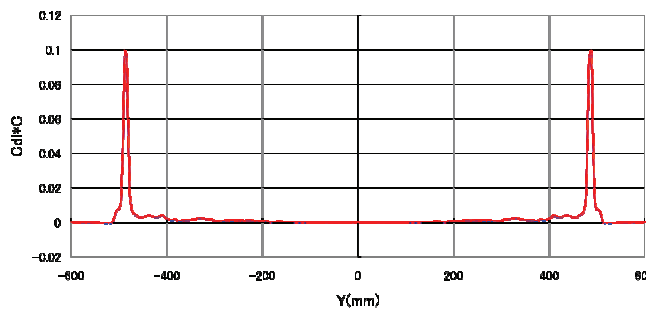


Figure 10 multi-plane stereo PIV results (U=30m/s, AoA=8deg).

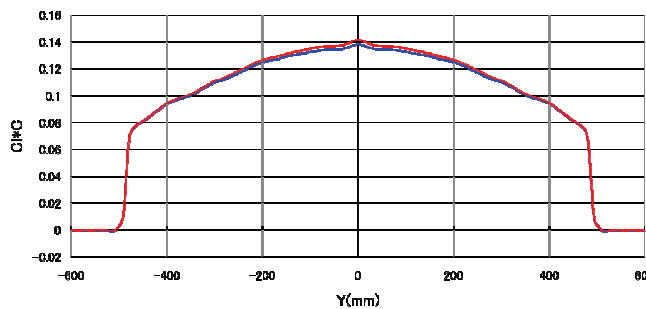


Figure 11 multi-plane stereo PIV results (U=30m/s, AoA=8deg).

## Conclusions

Pressure distribution is estimated from three velocity components at wake plane measured by stereo PIV system by CFD technique. It is development that the technique is applicable to wake integration method by means of velocity distribution measured by PIV and pressure distribution estimated by CFD

The wind tunnel testing was carried out in order to validate this technique. NACA0012 rectangle wing model was used in the wind tunnel testing. In the result, the drag estimated by PIV data is 0.01 differences from balance data due to the model supports. On the other hand, the lift estimated by PIV data is fairly good agreement with balance data, while the difference between PIV and balance is from 0.01 to 0.03. Also, the profile and induced drag estimation is qualitatively good results about wake plane distributions and spanwise distributions. Finally, It is demonstrated that profile and induced drag and lift force can be estimated by only PIV data.

## Acknowledgments

The authors are indebted to Junichi Akatsuka and Akiko Hidaka, Wind Tunnel Technology Center, JAXA. The authors are also indebted to the members of Low-Speed Wind Tunnel Section, Wind Tunnel Technology Center, JAXA for their support to the wind tunnel experiments and the data processing.

## References

- [1] Kusunose, K.: A Wake Integration method for Airplane Drag Prediction, Tohoku University Pres., 2005.
- [2] Aso, T., Matsushima, K. Nakahashi, K.: CFD Pressure Estimation using PIV Data. Proceedings of 2006 KSAS-JSASS Joint International Symposium,,159-163, 2006.
- [3] Watanabe, S.; Kato, H.: Stereo PIV Applications to Large-Scale Low-Speed Wind Tunnels, AIAA Paper 2003-0919, 2003.
- [4] Ueno, M. Akatsuka, J. and Hidaka, A.: Drag Decomposition Analysis of CFD Data of the DLR-F6 Model, AIAA Paper2008-6903, 2008.